Contemporary Mathematics

H1:01 H1:02

# Infinitesimally Locked Self-Touching Linkages with Applications to Locked Trees

H1:03 Robert Connelly, Erik D. Demaine, and Günter Rote

Abstract. Recently there has been much interest in linkages (bar-and-joint frameworks) that are *locked* or *stuck* in the sense that they cannot be moved into some other configuration while preserving the bar lengths and not crossing any bars. We propose a new algorithmic approach for analyzing whether planar linkages are locked in many cases of interest. The idea is to examine *self-touching* or *degenerate* frameworks in which multiple edges converge to geometrically overlapping configurations. We show how to study whether such frameworks are locked using techniques from rigidity theory, in particular first-order rigidity and equilibrium stresses. Then we show how to relate locked self-touching frameworks to locked frameworks that closely approximate the self-touching frameworks. Our motivation is that most existing approaches to locked linkages are based on approximations to self-touching frameworks. In particular, we show that a previously proposed locked tree in the plane [**BDD+02**] can be easily proved locked using our techniques, instead of the tedious arguments required by standard analysis. We also present a new locked tree in the plane with only one degree-3 vertex and all other vertices degree 1 or 2. This tree can also be easily proved locked with our methods, and implies that the result about opening polygonal arcs and cycles [**CDR02**] is the best possible.

H1:04

## 1. Linkages

H1:05 H1:06 H1:07 H1:08 H1:09 H1:10 H1:11 H1:12 H1:13 H1:14 H1:15 H1:16 H1:17 H1:18

A *linkage* is a graph together with an assignment of lengths to edges; each edge is called a rigid *bar*. We highlight three linkages of common study: a *polygonal arc*, *polygonal cycle*, or *polygonal tree* is a linkage whose graph is a single path, cycle, or tree, respectively. A *configuration* of a linkage in $\mathbb{R}^d$ is a mapping of the vertices to points in $\mathbb{R}^d$ that satisfies the bar-length constraints. A configuration is (*strongly*) *simple* if only incident bars intersect, and then only at the common endpoint. A *motion* is a continuum of configurations, that is, a continuous function mapping the time interval $[0, 1]$ to configurations; often, each configuration is required to be simple. The *configuration space* of a given subset of configurations (e.g., simple configurations) is the space in which points correspond to configurations and paths correspond to motions.

We focus here on *planar linkages* embedded in $\mathbb{R}^2$. In this case, the linkage also specifies the combinatorial planar embedding because this cannot change by a motion that avoids crossings. It is known that the configuration space of simple

H1:19 2000 *Mathematics Subject Classification.* Primary: 52C25.



©2002 American Mathematical Society

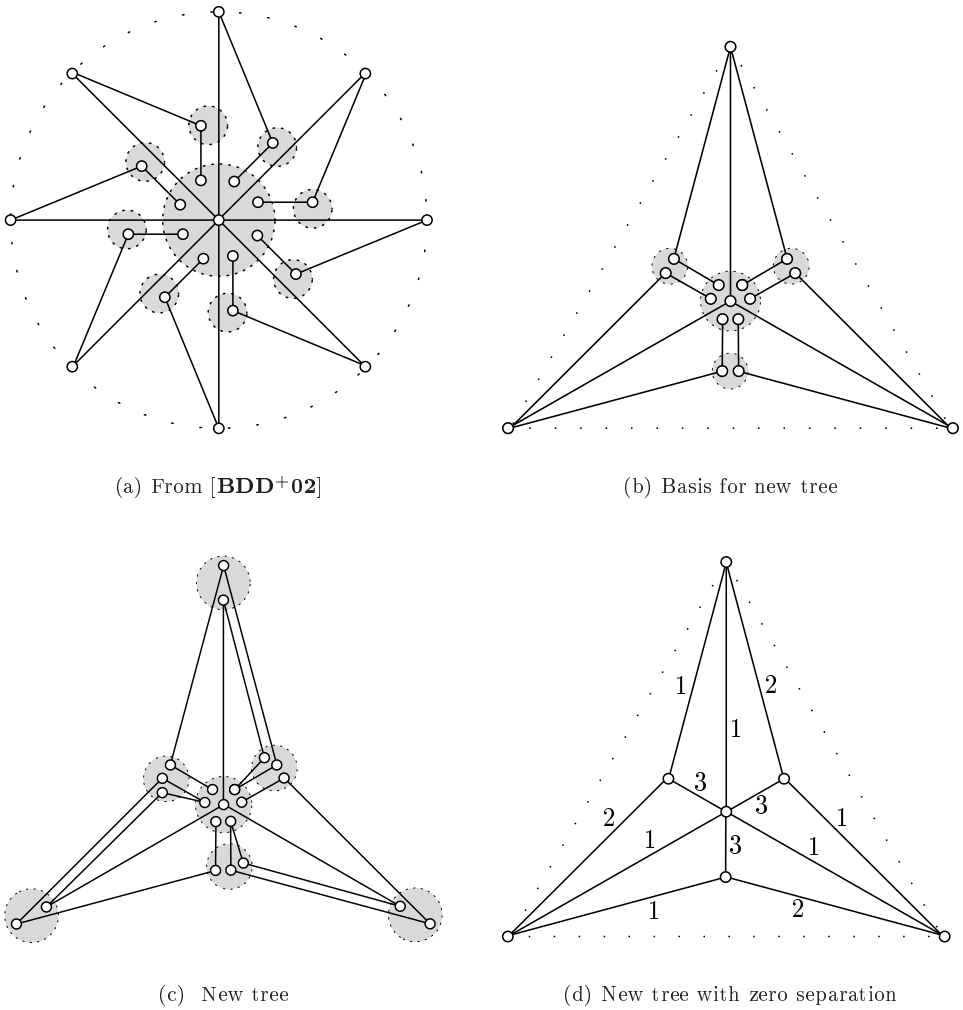


(a) From [**BDD+02**]

(b) Basis for new tree

(c) New tree

(d) New tree with zero separation

FIGURE 1. Locked planar polygonal trees. Points in dotted circles are closer than they appear.

H2:01 planar configurations is not always connected for a polygonal tree, as exemplified
H2:02 by the pinwheel tree in Figure 1(a) [**BDD+02**], and is always connected for a
H2:03 polygonal arc, polygonal cycle (up to reflection), and disjoint union of nonnested
H2:04 polygonal arcs and cycles [**CDR02, Str00**]. The key distinction is that arcs and
H2:05 cycles have maximum degree 2, but a tree may have vertices of higher degree.
H2:06 See [**CDR02, Dem00, O'R98**] for surveys of related results.

H2:07 Two questions naturally arise from these results.

H2:08 First, how many high-degree vertices are necessary, and how high must the
H2:09 degrees be, to make a tree have a disconnected configuration space? For example,
H2:10 the pinwheel tree in Figure 1(a) can be made to have a single degree-5 vertex, or
H2:11 three degree-3 vertices [**BDD+02**]. We settle this question by proving that the

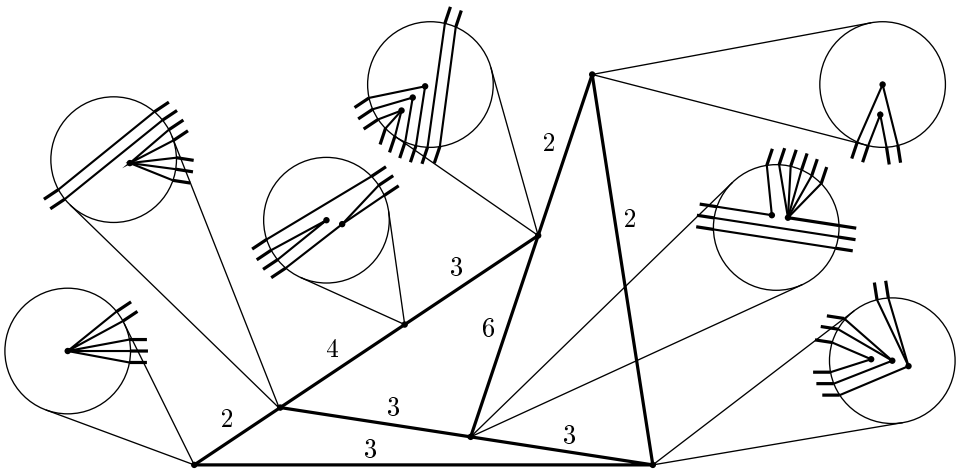


FIGURE 2. A self-touching linkage with 14 vertices and 21 edges. Numbers denote edge multiplicities.

H3:01 maximum-degree-2 result [**CDR02**] is tight: a single degree-3 vertex can prevent
H3:02 opening. See Figures 1(b) and 1(c) for the two-step construction.
H3:03 Second, and more generally, how can we tell whether a linkage has a connected
H3:04 configuration space? The best general algorithmic result for this problem is to
H3:05 use the roadmap algorithm for general motion planning [**Can87, Can88**], which
H3:06 runs in polynomial space but exponential time. We present a method for designing
H3:07 examples that can be proved without much effort to have a disconnected configura-
H3:08 tion space, and furthermore to be *strongly locked* in the sense that the tighter the
H3:09 linkage is constructed, the less freedom it has to move. This result does not settle
H3:10 the algorithmic decision problem, but solves many cases of interest. In particular,
H3:11 we use this result in our solution to the first problem.

## H3:12 2. Self-Touching Linkages

H3:13 Here we begin the exploration of the analogous linkage problems when bars
H3:14 are allowed to touch, and even lie along each other, but not properly cross. (A
H3:15 *proper crossing* is an intersection between the relative interiors of two nonparallel
H3:16 segments.) Our notion of self-touching linkage is an idealization because vertices
H3:17 and edges have no thickness. However, as we shall see, self-touching linkages can
H3:18 be used as a tool for studying properties of (more realistic) simple configurations
H3:19 of linkages.
H3:20 When we draw a geometric configuration of a self-touching linkage, several
H3:21 vertices and/or bars may coincide. (Such configurations are sometimes called *weakly*
H3:22 *simple*.) Thus, in addition to the geometric embedding, we require topological
H3:23 information to clarify the relationship between touching vertices and bars.
H3:24 More precisely, a *self-touching configuration* is defined as follows. We start with
H3:25 a plane straight-line graph $P$; see Figure 2 for an example. Each segment (edge) is
H3:26 marked with its *multiplicity*, that is, how many collinear bars lie along that segment.
H3:27 In addition, for each vertex, we add a microscopic *magnified view* enclosed by a
H3:28 circle. *Terminal points* on the boundary of the circle represent connections to the

H4:01 incident edges. Inside the circle, the terminals are connected by a plane graph, not
H4:02 necessarily drawn with straight-line edges, subject to the following rules:

H4:03 (1) Every terminal is incident to exactly one edge.
H4:04 (2) Every nonterminal vertex is incident to at least one edge.
H4:05 (3) There is at least one nonterminal vertex.
H4:06 (4) An edge may connect two terminals directly only if the terminals connect
H4:07 to two collinear segments that go in opposite directions.
H4:08 (5) All other edges must connect a terminal to a nonterminal vertex. In
H4:09 particular, no edge connects two nonterminal vertices.

H4:10 This structure specifies the combinatorial *linkage* associated with the configu-
H4:11 ration as follows. Its vertices are the nonterminal vertices in all circles. Its edges
H4:12 are the connections between those vertices; a single edge is a sequence starting
H4:13 and ending at a connection between a nonterminal and a terminal, and alternating
H4:14 between one or more additional segments and zero or more connections between
H4:15 terminals. We require in addition that the linkage has no duplicate edges.

H4:16 Figure 1(d) shows the multiplicities for the tree of Figure 1(c). We will not
H4:17 always use this representation in our figures; rather, we will use a schematic drawing
H4:18 where parallel edges are slightly separated, and dotted circles surround vertices
H4:19 that belong together in one point, as in Figure 1(c). This representation gives a
H4:20 clearer drawing of the underlying graph, and is closely linked to the concept of a
H4:21 $\delta$-perturbation defined in Section 4 below.

## H4:22 3. Self-Touching Configuration Space

H4:23 The *configuration space* is a space in which points correspond to self-touching
H4:24 configurations of a linkage as defined in the previous section, and paths correspond
H4:25 to motions of that linkage which keep edge lengths fixed and where no vertex or
H4:26 edge crosses through another edge. Before we examine the configuration space
H4:27 more carefully, note that a motion of a self-touching linkage can never change the
H4:28 *combinatorial embedding* of the linkage as a plane graph, i.e., the cyclic counter-
H4:29 clockwise sequence of edges around each vertex. (In addition, for graphs which
H4:30 are not connected, the combinatorial embedding also specifies the faces (cycles of
H4:31 edges) shared by several components.)

H4:32 The geometry of a configuration can be naturally represented by a vector $\mathbf{p} =$
H4:33 $(\mathbf{p}_1, \ldots, \mathbf{p}_n) \in \mathbb{R}^{2n}$, listing all coordinates for the $n$ vertices in the linkage. It will
H4:34 be convenient to define the *distance* between two configurations $\mathbf{p}$ and $\mathbf{q}$ as the
H4:35 maximum Euclidean distance in the plane between corresponding points:

H4:36 $$\|\mathbf{p} - \mathbf{q}\| = \max_{1 \le i \le n} \|\mathbf{p}_i - \mathbf{q}_i\|_2. \tag{3.1}$$

H4:37 Throughout the paper, $r_0$ denotes the minimum edge length, and $r_1 > 0$ is the
H4:38 minimum nonzero distance between two vertices or between a vertex and an edge,
H4:39 in a given configuration.

H4:40 A *motion* of a linkage with geometry $\mathbf{p}$ is specified by a continuous function
H4:41 $\mathbf{p}(t)$, $0 \le t \le T$ for some $T > 0$, with $\mathbf{p}(0) = \mathbf{p}$. Geometrically, such a motion must
H4:42 preserve the lengths of the bars:

H4:43 $$\|\mathbf{p}_i(t) - \mathbf{p}_j(t)\| = \|\mathbf{p}_i - \mathbf{p}_j\| \quad \text{for every bar } \{i, j\}. \tag{3.2}$$

H4:44 In addition, topologically, the relative positions of the parts of the linkage must
H4:45 remain *consistent*. For example, a vertex that touches an edge from the left side

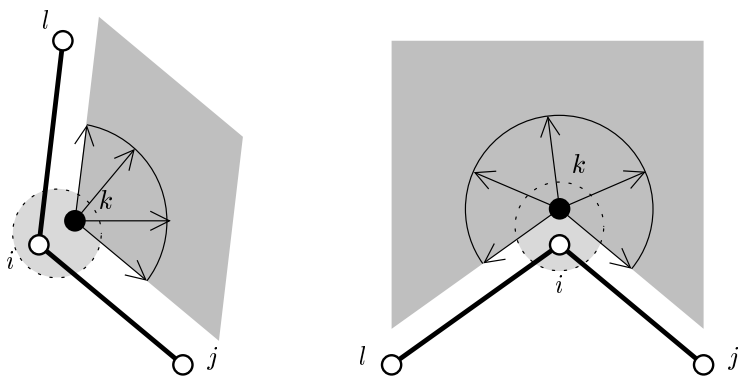


(a) Convex $\varphi \leq 180°$ (b) Reflex $\varphi > 180°$

FIGURE 3. Possible motions of vertex $\mathbf{p}_k$ (filled circle) relative to vertex $\mathbf{p}_i$ (empty circle).

H5:01 cannot suddenly move away to the right side of that edge. We shall now make
H5:02 this notion precise, and show how the set of feasible motions can be described by
H5:03 equations and inequalities, which are stable at least in some neighborhood of a given
H5:04 self-touching configuration. This development will be somewhat technical, and the
H5:05 reader who is satisfied with an intuitive understanding of self-touching linkages is
H5:06 encouraged to skip the rest of this section on first reading. The lemmas below are
H5:07 however important for the proofs in the rest of the paper.

H5:08 **3.1. Vertex-edge sidedness constraints.** First of all, we must forbid a ver-
H5:09 tex $\mathbf{p}_k$ from going through the middle of an edge $\mathbf{p}_i\mathbf{p}_j$: if $\mathbf{p}_k$ lies close to the edge
H5:10 but far enough from the endpoints $\mathbf{p}_i$ and $\mathbf{p}_j$, then $\mathbf{p}_k$ must remain on the same
H5:11 side of the edge, at least in some neighborhood of the current configuration. After
H5:12 possibly switching $i$ and $j$, we can express this constraint by saying that the point
H5:13 $\mathbf{p}_k$ must remain *on the left side* of the directed line through $\mathbf{p}_i$ and $\mathbf{p}_j$ or *on* this
H5:14 line. We denote this *vertex-edge sidedness constraint* by $L(i, j; k)$. It can be written
H5:15 using the determinant expression for the signed area of the triangle $\mathbf{p}_i\mathbf{p}_j\mathbf{p}_k$:

H5:16 $$\text{area}(\triangle \mathbf{p}_i\mathbf{p}_j\mathbf{p}_k) \geq 0. \tag{3.3}$$

H5:17 Globally, we select all pairs of a vertex $\mathbf{p}_k$ and an edge $\mathbf{p}_i\mathbf{p}_j$ where the distance
H5:18 between $\mathbf{p}_k$ and the edge is at most $r_0/2$, but the distances $\|\mathbf{p}_k - \mathbf{p}_i\|$ and $\|\mathbf{p}_k - \mathbf{p}_j\|$
H5:19 are both larger than $r_0/2$. Then the side of the line $\mathbf{p}_i\mathbf{p}_j$ containing $\mathbf{p}_k$ is uniquely
H5:20 determined, and these inequalities must be fulfilled by feasible motions, as long as
H5:21 no vertex moves $r_0/4$ or more from its initial position.

H5:22 **3.2. Vertex-chain noncrossing constraints.** When $\mathbf{p}_k$ is close to an end-
H5:23 point of an edge $\mathbf{p}_i\mathbf{p}_j$, we must formulate the constraint more carefully. Suppose
H5:24 that $\mathbf{p}_k$ moves in the vicinity of $\mathbf{p}_i$. Vertex $k$ lies in a wedge between two consecu-
H5:25 tive edges around vertex $i$; see Figure 3. if $\mathbf{p}_k$ is close enough to $\mathbf{p}_i$, this wedge is
H5:26 either determined by the geometry, or, if $\mathbf{p}_k = \mathbf{p}_i$, by the combinatorial information
H5:27 of the self-touching configuration.

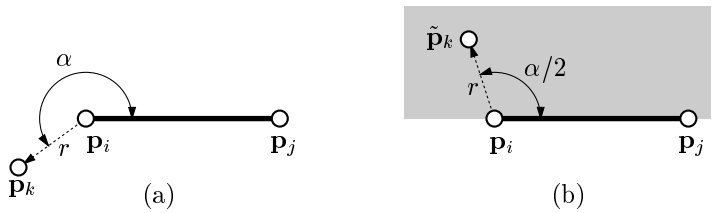


FIGURE 4. (a) The motion of $\mathbf{p}_k$ relative to $\mathbf{p}_i\mathbf{p}_j$. (b) The point $\tilde{\mathbf{p}}_k$ which is used to reparametrize the motion of $\mathbf{p}_k$, and the permitted area for $\tilde{\mathbf{p}}_k$ (shaded).

H6:01 Call the two consecutive edges of the wedge $\{j,i\}$ and $\{i,l\}$, so that vertex $k$
H6:02 lies in the counterclockwise wedge $j,i,l$. Then $\mathbf{p}_k$ is restricted to remain in this
H6:03 wedge. As a special case, vertex $i$ may be incident to only one edge, in which case
H6:04 the two edges bounding the wedge are the same, i.e., $j = l$.

H6:05 Let us first concentrate on the motion of $k$ relative to the edge $\mathbf{p}_i\mathbf{p}_j$. Vertex $k$
H6:06 can move freely but when it lies *on* the edge we must know on which side it lies.
H6:07 This cannot be distinguished on the basis of the coordinates alone. In order to
H6:08 write algebraic conditions for the feasible motions, we represent $\mathbf{p}_k$ in relative polar
H6:09 coordinates $r = \|\mathbf{p}_k - \mathbf{p}_i\|$ and the counterclockwise angle $\alpha$ between $\mathbf{p}_i\mathbf{p}_j$ and
H6:10 $\mathbf{p}_i\mathbf{p}_k$, $0 \le \alpha \le 2\pi$. See Figure 4. We now introduce a "shadow vertex" $\tilde{\mathbf{p}}_k = \tilde{\mathbf{p}}_{k,ij}$
H6:11 with the same distance $r$ but with polar angle $\alpha/2$. This point is confined to the left
H6:12 half-plane of the line through $\mathbf{p}_i, \mathbf{p}_j$, disambiguating the cases $\alpha = 0$ and $\alpha = 2\pi$.

H6:13 The relation between $\tilde{\mathbf{p}}_k$ and $\mathbf{p}_k$ can be described by algebraic equations by
H6:14 using the rotation matrix $\left(\begin{smallmatrix} c & -s \\ s & c \end{smallmatrix}\right)$ with $c = \cos(\alpha/2)$ and $s = \sin(\alpha/2)$:

H6:15
$$\tilde{\mathbf{p}}_k - \mathbf{p}_i = r \begin{pmatrix} c & -s \\ s & c \end{pmatrix} (\mathbf{p}_j - \mathbf{p}_i) \cdot \frac{1}{\|\mathbf{p}_j - \mathbf{p}_i\|}$$

H6:16
$$\mathbf{p}_k - \mathbf{p}_i = r \begin{pmatrix} c & -s \\ s & c \end{pmatrix}^2 (\mathbf{p}_j - \mathbf{p}_i) \cdot \frac{1}{\|\mathbf{p}_j - \mathbf{p}_i\|}$$

H6:17
$$c^2 + s^2 = 1,\ r \ge 0,$$

H6:18 By noting that the sidedness constraint on $\tilde{\mathbf{p}}_k$ translates to $s \ge 0$ and by absorbing
H6:19 the factors $r$ and $\frac{1}{\|\mathbf{p}_j - \mathbf{p}_i\|}$ into $c$ and $s$ we get the simpler parameterization

H6:20 (3.4)
$$\mathbf{p}_k - \mathbf{p}_i = \begin{pmatrix} a & -b \\ b & a \end{pmatrix}^2 (\mathbf{p}_j - \mathbf{p}_i), \quad a \in \mathbb{R},\ b \ge 0,$$

H6:21 using just two additional parameters $a$ and $b$ and eliminating $\tilde{\mathbf{p}}_k$ altogether.

H6:22 We can extend this formulation to include vertex $l$ also and write

(3.5)
$$\begin{cases} \mathbf{p}_l - \mathbf{p}_i = \begin{pmatrix} \bar{a} & -\bar{b} \\ \bar{b} & \bar{a} \end{pmatrix}^2 (\mathbf{p}_j - \mathbf{p}_i) \\ \mathbf{p}_k - \mathbf{p}_i = \begin{pmatrix} a & -b \\ b & a \end{pmatrix}^2 (\mathbf{p}_j - \mathbf{p}_i) \\ a, \bar{a} \in \mathbb{R},\ b, \bar{b} \ge 0, \quad a\bar{b} \le \bar{a}b \end{cases}$$

H6:23 using parameters $\bar{a}, \bar{b}, a, b$. The parameters $\bar{a}$ and $\bar{b}$ represent $\mathbf{p}_l$ relative to the edge
H6:24 $\mathbf{p}_i\mathbf{p}_j$ in the same way as $a$ and $b$ represent $\mathbf{p}_k$, and the last condition, $a\bar{b} \ge \bar{a}b$,

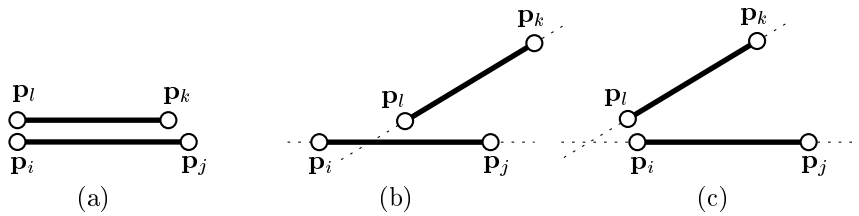


FIGURE 5. Two edges with coincident endpoints.

H7:01 essentially amounts to $a : b \leq \bar{a} : \bar{b}$, i.e., the counterclockwise angle $\mathbf{p}_j\mathbf{p}_i\mathbf{p}_k$ is
H7:02 bounded by the angle $\mathbf{p}_j\mathbf{p}_i\mathbf{p}_l$.

H7:03 The above condition remains valid as long as $\mathbf{p}_k$ does not cross the rays $\mathbf{p}_i\mathbf{p}_j$
H7:04 or $\mathbf{p}_i\mathbf{p}_l$ by going around $\mathbf{p}_j$ or $\mathbf{p}_l$.

H7:05 Globally, we look at each ordered pair of vertices $i, k$ with $\|\mathbf{p}_i - \mathbf{p}_k\| \leq r_0/2$,
H7:06 where $r_0$ is the minimum edge length, and we write condition (3.5) with the four
H7:07 new parameters $a_{ik}, \bar{a}_{ik} \in \mathbb{R}$ and $b_{ik}, \bar{b}_{ik} \geq 0$. We call these conditions the *vertex-*
H7:08 *chain noncrossing conditions*. Together with the vertex-edge sidedness conditions
H7:09 (3.3), these equations and inequalities are necessary and sufficient to describe the
H7:10 motions for which no vertex moves through a chain of edges (either in the middle
H7:11 of an edge or at a vertex), as long as no vertex moves $r_0/4$ or more from its initial
H7:12 position.

H7:13 When $i$ is incident to only one edge, or more generally, when all incident edges
H7:14 point in the same direction, constraint (3.5) does not restrict the positions that $\mathbf{p}_k$
H7:15 may reach, but does restrict the motions for getting there, preventing the point $\mathbf{p}_k$
H7:16 from crossing these edges.

H7:17 **3.3. Edge-edge sidedness constraints.** The constraints so far still do not
H7:18 prevent an edge from moving through another edge when some endpoints of the
H7:19 two edges coincide. If two edges $\mathbf{p}_i\mathbf{p}_j$ and $\mathbf{p}_k\mathbf{p}_l$ share an endpoint $\mathbf{p}_i = \mathbf{p}_l$, as
H7:20 in Figure 5(a), they might swap sides without any vertex going through an edge.
H7:21 So we formulate an explicit sidedness condition to specify that one edge must lie
H7:22 completely on the left side of the line through the other edge:

H7:23 $$\big(L(i,j;k) \wedge L(i,j;l)\big) \vee \big(L(k,l;i) \wedge L(k,l;j)\big) \tag{3.6}$$

H7:24 The correctness of this condition can be seen by considering the possibilities how
H7:25 the lines through the two segments can intersect each other, see Figure 5(b–c). We
H7:26 call these conditions the *edge-edge sidedness conditions*.

H7:27 Again, condition (3.6) is only valid as long as the points are sufficiently close
H7:28 to the critical configuration of Figure 5(a). So we write condition (3.6) for all
H7:29 pairs of edges $\mathbf{p}_i\mathbf{p}_j$ and $\mathbf{p}_k\mathbf{p}_l$ with $\|\mathbf{p}_i - \mathbf{p}_l\| < r_0/2$ (after a suitable relabeling).
H7:30 Then, as long as no vertex moves more than $r_0/4$ from its initial position, these
H7:31 conditions (3.6) are necessary and sufficient to prevent illegal movements of the
H7:32 involved edges.

H7:33 **3.4. Local characterizations of the configuration space.** We can now
H7:34 verify that the above conditions are sufficient to characterize the feasible motions in
H7:35 some neighborhood of a given configuration. The possibilities of one vertex crossing
H7:36 through another chain of edges at the interior of an edge or at an interior vertex

H8:01 are excluded by conditions (3.3) and (3.5), respecitively. Condition (3.6) deals with
H8:02 the remaining special case of two endpoints of two chains. We summarize this
H8:03 discussion in a lemma:

H8:04 LEMMA 3.1. *Let $r_0$ be the minimum edge length of a self-touching linkage with*
H8:05 *coordinate vector $\mathbf{p}^*$. Consider a path $\mathbf{p}(t) \in \mathbb{R}^{2n}$, $0 \le t \le T$ with $\mathbf{p}(0) = \mathbf{p}^*$,*
H8:06 *within the $r_0/4$-neighborhood of $\mathbf{p}^*$:*

H8:07 $$\|\mathbf{p}(t) - \mathbf{p}^*\| < r_0/4, \text{ for all } 0 \le t \le T$$

H8:08 *This path represents a feasible motion in the configuration space of self-touching*
H8:09 *linkages if and only if all bar lengths remain fixed* (3.2) *and all vertex-edge sided-*
H8:10 *ness conditions* (3.3)*, all vertex-chain noncrossing conditions* (3.5)*, and all edge-*
H8:11 *edge sidedness conditions* (3.6) *are satisfied, for all points $\mathbf{p} = \mathbf{p}(t)$, $0 \le t \le T$.*
H8:12 *(For the vertex-chain noncrossing conditions* (3.5)*, we must consider the motion*
H8:13 *in the space $\hat{\mathbf{p}}(t) \in \mathbb{R}^{2n+4m}$, for some $m$, which includes the additional parameters*
H8:14 *$\bar{a}_{ik}, \bar{b}_{ik}, a_{ik}, b_{ik}$.)* □

H8:15 Given that we have not formally defined the configuration space, one could
H8:16 also use this lemma as a *definition* of the configuration space. It provides a local
H8:17 coordinatization and algebraic description of the $r_0/4$-neighborhood of any given
H8:18 configuration, essentially covering the configuration space by balls of constant size
H8:19 in which the structure of the configuration space is explicitly given.

H8:20 The lemma also shows that, locally, the configuration space has the structure
H8:21 of a semi-algebraic set, i.e., a set defined by a Boolean combination of polynomial
H8:22 equations and inequalities.

H8:23 A more local characterization is possible by considering only those constraints
H8:24 that are *active*, i.e., coming from vertices that actually lie *on* an edge or another
H8:25 vertex. A vertex-edge sidedness condition (3.3) is active when $\mathbf{p}_k$ touches the
H8:26 interior of the edge $\mathbf{p}_i\mathbf{p}_j$ but does not coincide with an endpoint $\mathbf{p}_i$ or $\mathbf{p}_j$. (In
H8:27 contrast to Lemma 3.1, we do not care about the distance $\|\mathbf{p}_k - \mathbf{p}_i\|$ or $\|\mathbf{p}_k -$
H8:28 $\mathbf{p}_j\|$ when we define whether the constraint is active.) A vertex-chain noncrossing
H8:29 condition (3.5) is active if $\mathbf{p}_i = \mathbf{p}_k$. Finally, an edge-edge sidedness condition (3.6)
H8:30 is active if $\mathbf{p}_i = \mathbf{p}_j$ *and* the two edges $\mathbf{p}_i\mathbf{p}_j$ and $\mathbf{p}_l\mathbf{p}_k$ are parallel and point in the
H8:31 same direction. An inactive constraint does not restrict a motion that is so small
H8:32 that the constraint cannot possibly become active. This threshold is determined by
H8:33 the minimum nonzero distance $r_1$ between two vertices or between a vertex and an
H8:34 edge, in a given configuration. Unlike $r_0$, this quantity may depend on the given
H8:35 configuration. We have the following direct corollary of Lemma 3.1.

H8:36 LEMMA 3.2. *Let $r_1$ be the minimum positive distance between two vertices or*
H8:37 *between a vertex and an edge in a given self-touching configuration. with coordinate*
H8:38 *vector $\mathbf{p}^*$. Consider a path $\mathbf{p}(t) \in \mathbb{R}^{2n}$, $0 \le t \le T$ and with $\mathbf{p}(0) = \mathbf{p}^*$, within the*
H8:39 *$r_1/2$-neighborhood of $\mathbf{p}^*$. This path represents a feasible motion in the configuration*
H8:40 *space of self-touching linkages if and only if all bar lengths remain fixed and all active*
H8:41 *conditions* (3.3)*,* (3.5)*, and* (3.6) *are satisfied for all points $\mathbf{p} = \mathbf{p}(t)$, $0 \le t \le T$.* □

H8:42 The set of constraints in the lemma can be simplified for practical purposes, by
H8:43 looking at the combination of several conditions which restrict the relative motion
H8:44 of two vertices. We will make a few of these simplifications later in Section 6 when
H8:45 we consider the infinitesimal motions of a given configuration.

## 4. Locked Linkages

*Locked configurations.* There are two basic notions of being "locked"; the first notion is the most commonly defined in previous work, but the second notion better captures the intended essence of previous examples. (1) We call a self-touching linkage *locked* if the configuration space has multiple connected components within the class of embeddings with the same combinatorial planar embedding. (2) We call a self-touching configuration *locked within* $\varepsilon$ if no path in the configuration space (motion) can get outside of a surrounding ball of radius $\varepsilon$. The second definition is stronger for sufficiently small $\varepsilon$, provided that there are other configurations which represent the same combinatorial embedding.

*Rigid configurations.* One instance of the second definition is the following: a self-touching configuration is called *rigid* if it is locked within 0, that is, there is no motion to a distinct self-touching configuration. This notion is not useful for simple configurations of arcs, cycles, and trees, which are always *flexible* (not rigid). One key feature of self-touching configurations of such linkages is that they can be rigid; other examples of rigid configurations that arise throughout rigidity theory are linkages that form a complex graph structure (consisting of multiple cycles).

*Perturbations.* To introduce a stronger notion of being locked, we give the following definition. A *$\delta$-perturbation* of a self-touching configuration is a repositioning of the vertices within disks of radius $\delta$ that remains consistent with the combinatorial description defined in Section 2. More precisely, for $\delta < r_1/2$, a $\delta$-perturbation must satisfy all active constraints given in Lemma 3.2. A key aspect of a perturbation is that it allows the bar lengths to change slightly (each by at most $2\delta$).

CONJECTURE 4.1. *For every self-touching configuration and for every $\delta > 0$, there is a $\delta$-perturbation that is a simple configuration.*

From the definition we can easily obtain a representation where every edge is represented by a polygonal arc, but it seems difficult to simultaneously straighten these arcs.

*Strongly locked configurations.* Now, a self-touching configuration is *strongly locked* if, for every $\varepsilon > 0$, there is a $\delta > 0$ such that every $\delta$-perturbation is locked within $\varepsilon$. In particular, all sufficiently small simple perturbations are locked. Thus, assuming Conjecture 4.1, the definition of strongly locked configurations provides a connection between the less-intuitive notion of self-touching configurations and the more commonly studied notion of simple configurations. Typically, in particular for the examples considered here, the self-touching configuration arises naturally from a simple configuration, so we need not rely on Conjecture 4.1.

Our goal is to connect strongly locked configurations to notions in rigidity theory which are described in the next section.

## 5. Rigidity Background

The notions of rigidity, infinitesimal rigidity, and equilibrium stresses are well-understood for *bar frameworks*, configurations of linkages whose bars are permitted to cross each other, and even *tensegrity frameworks* which contain struts and cables that can change their length only monotonically; see [**CDR02, AR78, AR79, Con80, Con82, Con93, CW96, CW93, CW82, CW94, GSS93, RW81, Whi84a, Whi84b, Whi87, Whi88, Whi92**]. This section gives a brief summary

H10:01 of the relevant material, so that we can generalize it to self-touching configurations
H10:02 of linkages whose bars cannot cross.

H10:03 *Rigidity.* A *motion* of a tensegrity framework $\mathbf{p}$ is a continuous function $\mathbf{p}(t)$,
H10:04 $0 \le t \le T$ for some $T > 0$, with $\mathbf{p}(0) = \mathbf{p}$, that preserves the bar lengths according
H10:05 to equation (3.2). A motion is *trivial* if it is a rigid motion (translation and/or
H10:06 rotation). A tensegrity framework $\mathbf{p}$ is *rigid* if it has no nontrivial motion. This
H10:07 definition is a variation of the definition of rigidity for self-touching linkages given
H10:08 in the previous section.

H10:09 *Infinitesimal rigidity.* A tensegrity framework is *infinitesimally rigid* if it has
H10:10 no *infinitesimal motion*, that is, assignment of velocity vectors $\mathbf{v}_i$ to vertices $\mathbf{p}_i$
H10:11 that preserves bar lengths to the first order:

H10:12 $$(\mathbf{p}_i - \mathbf{p}_j) \cdot (\mathbf{v}_i - \mathbf{v}_j) = 0 \quad \text{for every bar } \{i, j\}. \tag{5.1}$$

H10:13 Not every infinitesimal motion can be extended to a motion. Thus, rigidity does
H10:14 not imply infinitesimal rigidity, but the converse implication holds, since a suitable
H10:15 motion can be converted into an infinitesimal motion by taking the derivative at
H10:16 time 0:

H10:17 LEMMA 5.1. [**CW96, RW81**] *If a tensegrity framework is infinitesimally rigid,*
H10:18 *then it is rigid.*

H10:19 We will generalize this result to self-touching linkages in the next section.

H10:20 *Struts.* In addition to bars, a framework may have some edges marked as *struts*.
H10:21 The definitions above change as follows in the presence of struts. A motion can
H10:22 never decrease the length of a strut, but may now increase the length of a strut.
H10:23 An infinitesimal motion cannot decrease the length of a strut to the first order:

H10:24 $$(\mathbf{p}_i - \mathbf{p}_j) \cdot (\mathbf{v}_i - \mathbf{v}_j) \ge 0 \quad \text{for every strut } \{i, j\}. \tag{5.2}$$

H10:25 In addition to struts, tensegrity frameworks may also contain *cables*, whose change
H10:26 of length is restricted in the opposite direction. We will not use cables in this paper.
H10:27 Lemma 5.1 holds in the presence of struts and cables as well.

H10:28 *Equilibrium stress.* A classic duality result connects infinitesimally rigidity to
H10:29 "equilibrium stresses." A *stress* $\omega$ assigns a real number $\omega_{\{i,j\}}$ to each bar $\{i, j\}$ and
H10:30 a nonpositive real number $\omega_{\{i,j\}} \le 0$ to each strut $\{i, j\}$. Intuitively, if the stress
H10:31 is negative, then the bar or strut pulls on its endpoints by a force proportional to
H10:32 the stress; and if the stress is positive, then the bar pushes against the two ends by
H10:33 the same amount. A stress is *in equilibrium* if these forces add up to zero:

H10:34 $$\sum_j \omega_{\{i,j\}}(\mathbf{p}_j - \mathbf{p}_i) = 0, \quad \text{for every vertex } i. \tag{5.3}$$

H10:35 Infinitesimal rigidity is closely related to equilibrium stress:

H10:36 LEMMA 5.2. [**RW81**] *If a tensegrity framework is infinitesimally rigid, then it*
H10:37 *has an equilibrium stress that is nonzero on all struts and cables.*

H10:38 The converse of this lemma holds under an additional assumption:

H10:39 LEMMA 5.3. [**RW81**, Theorem 5.2] *If a tensegrity framework has an equilib-*
H10:40 *rium stress that is nonzero on all cables and struts, and the framework becomes*
H10:41 *infinitesimally rigid when each strut and cable is replaced by a bar, then the origi-*
H10:42 *nal framework is infinitesimally rigid.*

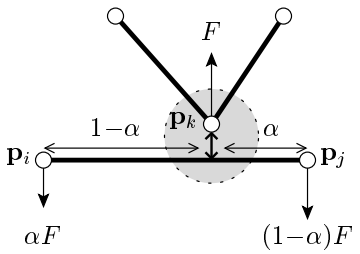


FIGURE 6. Sliding zero-length strut (small double arrow) and proportional distribution of stress $F$ (single arrows). Bold edges denote bars.

H11:01 *Connection to linear programming.* A useful feature of infinitesimal motions
H11:02 is that the bar constraints (5.1) and strut constraints (5.2) are linear equations
H11:03 and inequalities, where $\mathbf{p}$ is known and $\mathbf{v}$ is unknown, and hence can be solved
H11:04 via linear programming. If the linear program can be solved only by trivial (rigid)
H11:05 motions, then the configuration is infinitesimally rigid, and the dual linear program
H11:06 provides an equilibrium stress. (The stresses $\omega$ are precisely the dual variables.)
H11:07 This connection to linear programming is a property we will strive for in our setting.

## H11:08 6. Infinitesimal Motions for Self-Touching Linkages

H11:09 For simple configurations of linkages whose bars are not permitted to cross,
H11:10 the noncrossing constraint automatically holds for a sufficiently short interval of
H11:11 time, so the notions of rigidity and infinitesimal rigidity remain unchanged. For
H11:12 self-touching configurations, however, the noncrossing constraint introduces addi-
H11:13 tional restrictions at the very beginning of motion. Indeed, this property is the key
H11:14 advantage of self-touching configurations, and is what brings locked configurations
H11:15 into the realm of rigidity theory.
H11:16 The generalizations of motions and thus rigidity is straightforward: motions
H11:17 correspond to paths in the configuration space which has the additional restrictions
H11:18 described in Section 3. For infinitesimal motions, we need to determine the first-
H11:19 order noncrossing constraints. We will look at the active constraints specified in
H11:20 Lemma 3.2 and translate them into constraints on the velocities $\mathbf{v}_i$. They will turn
H11:21 out to be polyhedral (piecewise linear) constraints, but unfortunately, they are not
H11:22 always convex.

### H11:23 6.1. Vertices lying on an edge.

H11:24 *Sidedness constraint.* The simplest type of constraint arises when a vertex $\mathbf{p}_k$
H11:25 hits the relative interior of a bar $\mathbf{p}_i\mathbf{p}_j$, but not one of the bar's endpoints $\mathbf{p}_i$ or $\mathbf{p}_j$.
H11:26 See Figure 6. In the combinatorial description defined in Section 2, this situation
H11:27 arises when there is a terminal-terminal connection in the magnified view. This
H11:28 situation causes a vertex-edge sidedness constraint (3.3) which we have denoted by
H11:29 $L(i, j; k)$: $\mathbf{p}_k$ must remain on the left side of the line through $\mathbf{p}_i$ and $\mathbf{p}_j$.

H11:30 $$\text{area}(\triangle \mathbf{p}_i(t), \mathbf{p}_j(t), \mathbf{p}_k(t)) \geq 0. \tag{6.1}$$

H11:31 For infinitesimal motions, we take the derivative at time $t = 0$, noting that the
H11:32 expression is initially zero, and we get the following necessary condition:

H11:33 $$(\mathbf{p}_i - \mathbf{p}_j)^\perp \cdot \mathbf{v}_k + (\mathbf{p}_j - \mathbf{p}_k)^\perp \cdot \mathbf{v}_i + (\mathbf{p}_k - \mathbf{p}_i)^\perp \cdot \mathbf{v}_j \geq 0, \tag{6.2}$$

where $\binom{x}{y}^{\perp} = \binom{-y}{x}$ denotes a counterclockwise rotation by 90°.

Because the three vectors $(\mathbf{p}_j - \mathbf{p}_i)^{\perp}$, $(\mathbf{p}_i - \mathbf{p}_k)^{\perp}$, and $(\mathbf{p}_k - \mathbf{p}_j)^{\perp}$ are parallel, we can also denote this constraint differently, using the representation of $\mathbf{p}_k$ as a convex combination of $\mathbf{p}_i$ and $\mathbf{p}_j$, $\mathbf{p}_k = \alpha\mathbf{p}_i + (1-\alpha)\mathbf{p}_j$ with $0 < \alpha < 1$:

$$\mathbf{v}_k \cdot \mathbf{b} \geq (1-\alpha)\mathbf{v}_i \cdot \mathbf{b} + \alpha\mathbf{v}_j \cdot \mathbf{b} \quad \text{where } \mathbf{b} = (\mathbf{p}_j - \mathbf{p}_i)^{\perp} \tag{6.3}$$

We denote these constraints by $L'(i,j;k)$ and regard them as linear inequalities in the unknowns $\mathbf{v}$. The notation $L'$ reminds us that these constraints were obtained as a "derivative" of the constraints $L(i,j;k)$.

**6.2. Coincident vertices.** Consider two vertices $i$ and $k$ that coincide geometrically; refer to Figure 3. We begin by considering the constraints on $k$, and later return to the constraints on $i$. As discussed in Section 3.2, vertex $k$ lies in a wedge between two consecutive edges around vertex $i$. Call the edges $\{j,i\}$ and $\{i,l\}$, so that vertex $k$ lies in the counterclockwise wedge $j,i,l$. Let $\varphi$ denote the angle of the wedge. As a special case, vertex $i$ may be incident to only one edge, in which case the two edges bounding the wedge are the same, i.e., $j = l$, and $\varphi = 360°$.

By the vertex-chain noncrossing condition (3.5), the relative first-order movement $\mathbf{v}_k - \mathbf{v}_i$ of $\mathbf{p}_k$ with respect to $\mathbf{p}_i$, is restricted to the angular wedge between the two edges $\mathbf{p}_i\mathbf{p}_j$ and $\mathbf{p}_l\mathbf{p}_i$. For $\varphi \leq 180°$, we have a convex cone, which is described by the conjunction that $\mathbf{p}_k$ must remain to the left of the line $\mathbf{p}_i\mathbf{p}_j$ *and* to the left of the line $\mathbf{p}_l\mathbf{p}_i$ (Figure 3(a)):

$$L'(i,j;k) \wedge L'(l,i;k).$$

For a reflex angle $\varphi > 180°$, we have a nonconvex cone which is described by the disjunction that $\mathbf{p}_k$ must remain to the left of the line $\mathbf{p}_i\mathbf{p}_j$ *or* to the left of the line $\mathbf{p}_l\mathbf{p}_i$ (Figure 3b). We introduce a special notation for this condition

$$M'(i,j,l;k) \iff L'(i,j;k) \vee L'(l,i;k).$$

Note that it is not necessary to introduce the additional parameters $\bar{a}, \bar{b}, a, b$; we can remain in the original space $\mathbb{R}^{2n}$.

The vertex $j$ is restricted by a wedge defined by two consecutive edges around $k$ in the same way, giving rise to further conditions of the above form.

The infinitesimal versions of the edge-edge sidedness conditions (3.6) can be derived in the same way, giving rise to the single linear constraint $L'(i,j;l)$; see Figure 7(c). (The remaining conditions of (3.6) follow from the vertex-edge sidedness constraints.)

**6.3. Infinitesimal rigidity.** For the feasible directions of motion, we have given by a set $\mathcal{M}$ of necessary constraints of the form $L'(i,j;k)$ and $M'(i,j,l;k)$. For such a set $\mathcal{M}$ of constraints, we denote by $P_{\mathcal{M}}$ the set of infinitesimal motions $\mathbf{v}$ that satisfy those constraints and the length preservation equations (5.1). This set is a polyhedral cone. The linkage $\mathbf{p}$ is *infinitesimally rigid* if $P_{\mathcal{M}}$ contains only trivial infinitesimal motions. We have the following generalization of Lemma 5.1:

LEMMA 6.1. *If a self-touching configuration is infinitesimally rigid, then it is rigid.*

H13:01 PROOF. The proof can be given along the lines of a proof used in the context of
H13:02 "second-order rigidity" [**CW96**, Theorem 4.3.1] to show that second-order rigidity
H13:03 implies rigidity. We only sketch the main idea of the proof here. In a neighborhood
H13:04 of a self-touching configuration $\mathbf{p}$, a motion is confined within a semi-algebraic
H13:05 set defined by the equations and inequalities given in Lemma 3.1. Any point in
H13:06 a semi-algebraic set has a neighborhood with an analytic parameterization; see
H13:07 e.g. [**Mil68**]. Thus, if $\mathbf{p}$ is not rigid, we obtain a short analytic motion $\mathbf{p}(t)$ with
H13:08 $\mathbf{p}(0) = \mathbf{p}$. The tangent direction $\mathbf{v}$ at $\mathbf{p}$ (the first nonvanishing coefficient of the
H13:09 power-series expansion of $\mathbf{p}(t)$ at $t = 0$) is then an infinitesimal motion of $\mathbf{p}$. □

H13:10 **6.4. Reduction to convex cones.** Unfortunately, because of the nonconvex
H13:11 constraints $M'(i, j, l; k)$, $P_{\mathcal{M}}$ is in general not convex. In showing that $P_{\mathcal{M}}$ contains
H13:12 only rigid motions (and thus the framework is infinitesimally rigid), we would like
H13:13 to apply linear programming and the duality theory of convex cones.
H13:14 There are two options to reduce the problem to convex cones. First, we may
H13:15 take the *convex relaxation* by simply ignoring all disjunctive constraints of the form
H13:16 $M'(i, j, l; k)$:

H13:17 $$P_{\mathcal{M}} \subseteq P_{\mathcal{M}'},$$

H13:18 where $\mathcal{M}' \subseteq \mathcal{M}$ contains only the constraints of the form $L'(i, j; k)$. If we succeed
H13:19 in showing that this relaxed cone $P_{\mathcal{M}'}$ contains only the rigid motions, then so does
H13:20 the original cone and we are done.
H13:21 Second, we can represent the cone as a union of convex cones, by picking
H13:22 one $L$ inequality from each disjunction $M$ of inequalities, and trying all possible
H13:23 combinations. If we have $s$ disjunctions, we obtain $2^s$ convex cones:

H13:24 $$P_{\mathcal{M}} = P_{\mathcal{M}_1} \cup P_{\mathcal{M}_2} \cup P_{\mathcal{M}_3} \cup \cdots \cup P_{\mathcal{M}_{2^s}}$$

H13:25 Each of these cones is convex, so we can check the existence of nontrivial solutions
H13:26 in each of these cones by linear programming or by the techniques discussed in
H13:27 Section 7.
H13:28 We summarize the two approaches in a small lemma. We let $G_{\mathcal{M}}$ denote the
H13:29 tensegrity framework corresponding to the set of constraints $\mathcal{M}$.

H13:30 LEMMA 6.2. (1) *If $G_{\mathcal{M}'}(\mathbf{p})$ is infinitesimally rigid, then so is $G_{\mathcal{M}}(\mathbf{p})$.*
H13:31 (2) *$G_{\mathcal{M}}(\mathbf{p})$ is infinitesimally rigid if and only if all frameworks $G_{\mathcal{M}_1}(\mathbf{p}), \ldots,$*
H13:32 *$G_{\mathcal{M}_{2^s}}(\mathbf{p})$ are infinitesimally rigid.* □

H13:33 Any combination of the two approaches, like in a branch-and-bound tree, is
H13:34 also possible.
H13:35 In some instances, like in Figure 1(a), we do not have a vertex in a reflex
H13:36 wedge as in Figure 3b, and $P_{\mathcal{M}}$ is already a convex cone. But even in other cases,
H13:37 some simplifications are possible. If we look at two coincident vertices $j$ and $k$,
H13:38 we can combine $j$'s constraints and $k$'s constraints, and instead of two disjunctions
H13:39 of the form $M'(i, j, l; k)$ we get only one disjunction of two linear inequalities, or
H13:40 even convex constraints, as follows. When the two relevant angles at $\mathbf{p}_i$ and $\mathbf{p}_k$
H13:41 are both reflex, the direction of movement $\mathbf{v}_k - \mathbf{v}_i$ is constrained by two extreme
H13:42 directions which correspond to the two extreme directions of a line separating the
H13:43 two chains through $\mathbf{p}_i$ and $\mathbf{p}_k$ locally (Figures 7(a) and 7(b)). This constraint
H13:44 can be represented as a logical disjunction of two linear constraints of the form
H13:45 $L'(i, j; k)$, but not necessarily in the pattern given by $M'(i, j, l; k)$ above. There is
H13:46 one special case when two reflex angles meet but they nevertheless produce a single

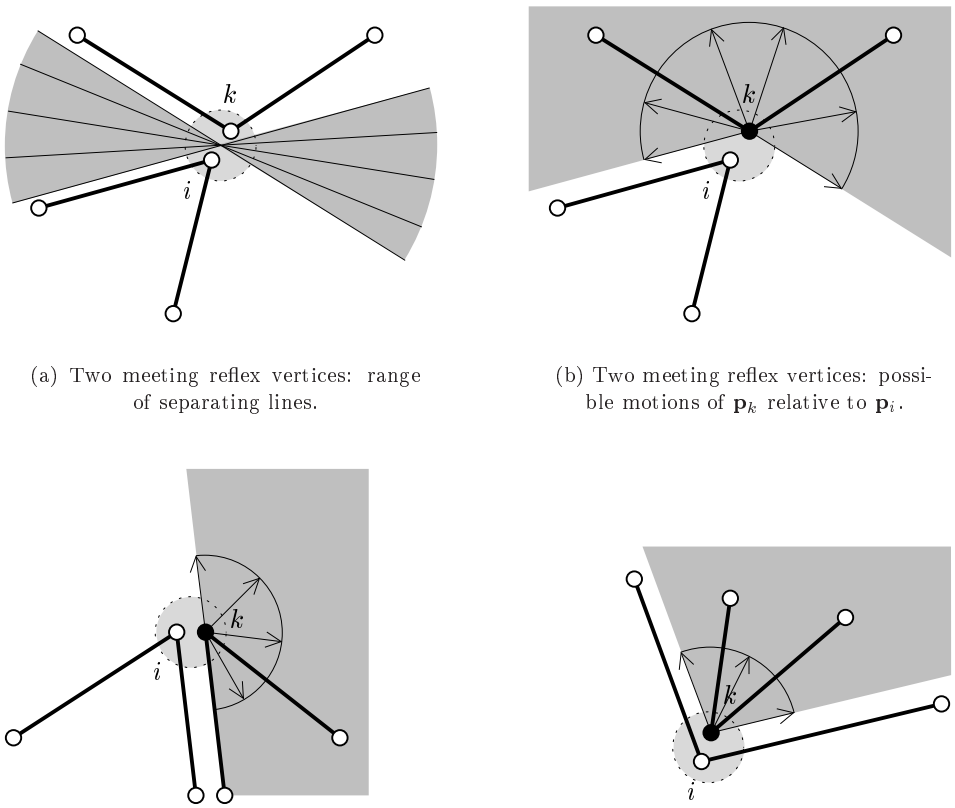


(a) Two meeting reflex vertices: range of separating lines.

(b) Two meeting reflex vertices: possible motions of $\mathbf{p}_k$ relative to $\mathbf{p}_i$.

(c) Two meeting reflex vertices sharing an edge direction.

(d) A convex vertex meeting a reflex vertex.

FIGURE 7. Cases of constraint interplay between touching vertices $\mathbf{p}_i$ and $\mathbf{p}_k$. The shaded area in (b), (c), and (d) indicates the range of possible motions of $\mathbf{p}_k$ relative to $\mathbf{p}_i$.

H14:01 inequality: when the two chains have two edges pointing in the same direction
H14:02 (Figure 7(c)). This is in fact just the infinitesimal version of the edge-edge sidedness
H14:03 conditions (3.6). Finally, when one chain lies inside a convex angle of the other
H14:04 chain, we get a convex wedge which is representable as a conjunction of two linear
H14:05 constraints (Figure 7(d)).

H14:06 It suffices to constrain only those pairs of touching vertices that are combi-
H14:07 natorially adjacent, that is, not obscured from each other by connections in the
H14:08 magnified view. This also eliminates a number of nonconvex constraints.

## H14:09 7. Stresses for Self-Touching Linkages

H14:10 In this section we assume that we have no constraints of the form $M'(i,j,l;k)$,
H14:11 and discuss how the sidedness constraints $L'(i,j;k)$ can be treated in using the
H14:12 notion of stresses.

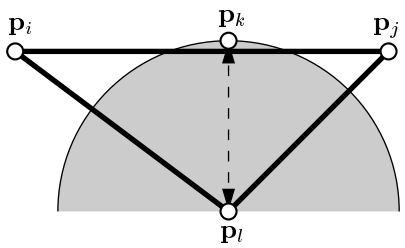


FIGURE 8. A construction replacing a sliding zero-length strut

H15:01 *Sliding zero-length struts.* The constraint $L'(i,j;k)$ can be viewed as a *sliding*
H15:02 *zero-length strut* with one end at $\mathbf{p}_k$ and the other end sliding along the bar $\mathbf{p}_i\mathbf{p}_j$
H15:03 to match the orthogonal projection of $\mathbf{p}_k$ onto the bar.
H15:04 *Modeling by tensegrity frameworks.* We can also model these conditions by an
H15:05 auxiliary vertex $\mathbf{p}_l$ and a "classic" strut; see Figure 8. Choose a point $\mathbf{p}_l$ on the line
H15:06 through $\mathbf{p}_k$ perpendicular to $\mathbf{p}_i\mathbf{p}_j$, on the opposite side of where $\mathbf{p}_k$ is constrained
H15:07 to lie. Connect $\mathbf{p}_l$ to $\mathbf{p}_k$ by a strut and to $\mathbf{p}_i$ and $\mathbf{p}_j$ by bars. Then keeping $\mathbf{p}_i$ and
H15:08 $\mathbf{p}_j$ fixed, the point $\mathbf{p}_k$ is prevented from entering the circle around $\mathbf{p}_l$ through $\mathbf{p}_k$.
H15:09 This condition is (locally) weaker than the original sidedness constraint $L'(i,j;k)$.
H15:10 In terms of directions (infinitesimal motions), however, it is equivalent. Thus we
H15:11 have the following statement:

H15:12 LEMMA 7.1. (1) *The augmented bar-and-strut framework is infinitesimally rigid*
H15:13 *if and only if the original self-touching linkage is infinitesimally rigid.*
H15:14 (2) *If the augmented bar-and-strut framework is rigid then the original self-*
H15:15 *touching linkage is rigid.* □

H15:16 We do not know whether equivalence holds for rigidity, too.
H15:17 *Stress.* The proper generalization of stresses for frameworks with sidedness con-
H15:18 straints may be derived in two ways. First, they are the dual variables corresponding
H15:19 to the infinitesimal sidedness constraints $L'(i,j;k)$; secondly, we may consult the
H15:20 stress in the augmented framework with the auxiliary network. Both approaches
H15:21 lead to the same intuitive result, as shown in Figure 6. A stress of $F = \omega_{k,ij} \leq 0$
H15:22 on a sliding strut induces a force of magnitude $-F$ on $\mathbf{p}_k$ perpendicular and to the
H15:23 left of bar $\mathbf{p}_i\mathbf{p}_j$, and the opposite force is distributed proportionally to $\mathbf{p}_i$ and $\mathbf{p}_j$
H15:24 based on their relative proximity to $\mathbf{p}_k$. More precisely, $\mathbf{p}_i$ feels a force of $-\alpha F$
H15:25 perpendicular and to the right of bar $\mathbf{p}_i\mathbf{p}_j$, and $\mathbf{p}_j$ feels a force of $-(1-\alpha)F$ per-
H15:26 pendicular to the right of bar $\mathbf{p}_i\mathbf{p}_j$. In an equilibrium stress, the sum of these forces
H15:27 at each vertex must leave the vertex stationary as in (5.3).
H15:28 *Connections between infinitesimal rigidity and equilibrium stress.* Lemmas 5.2
H15:29 and 5.3 can be directly applied to the tensegrity frameworks derived above with
H15:30 the auxiliary vertices. They can also be translated into the notions of sliding zero-
H15:31 length struts. We need to define a *sliding zero-length bar*: such a bar restricts $\mathbf{p}_k$
H15:32 to remain on (the left side of) the bar $\mathbf{p}_i\mathbf{p}_j$, but leaves $\mathbf{p}_k$ free to slide along the
H15:33 bar.

H15:34 LEMMA 7.2. *A self-touching configuration is infinitesimally rigid if and only if*
H15:35 *the following two conditions hold*:

H16:01 (1) *the configuration becomes infinitesimally rigid when each sliding zero-*
H16:02 *length strut is replaced by a sliding zero-length bar, and*
H16:03 (2) *the self-touching framework has a stress that is negative on every sliding*
H16:04 *zero-length strut.* □

H16:05 ## 8. Connection Between Rigid and Locked

H16:06 The relevance of the generalized rigidity theory developed in the previous sec-
H16:07 tion is the following connection between rigid and locked linkages:

H16:08 THEOREM 8.1. *If a self-touching configuration is rigid, then it is strongly locked.*

H16:09 In fact, we will show this result even when the $\delta$-perturbations are permitted
H16:10 to satisfy the bar and noncrossing constraints approximately, up to tolerance $2\delta$.
H16:11 This result is an extension of a result about "sloppy rigidity" [**Con82**, Theorem 1]
H16:12 stating essentially the same result (in different words) for tensegrity frameworks.
H16:13 Our proof follows the same outline. A different proof, working on the stronger
H16:14 assumption of *infinitesimal* rigidity, is given in the appendix. That proof, however,
H16:15 has the advantage of providing explicit bounds on $\delta$ in terms of $\varepsilon$.

H16:16 PROOF. The proof is based on a topological argument about closed sets of
H16:17 configurations and their neighborhoods.

H16:18 LEMMA 8.2. *Let $A_\delta \subseteq \mathbb{R}^m$ $(\delta \geq 0)$ be a family of closed sets with $A_\delta \subseteq A_{\delta'}$ for*
H16:19 *$0 \leq \delta < \delta'$ and*

H16:20 $$\bigcap_{\delta>0} A_\delta = A_0.$$

H16:21 *For $\mathbf{p} \in A_\delta$ we denote by $B_\delta(\mathbf{p})$ the set of points which are reachable by a curve*
H16:22 *in $A_\delta$ starting at $\mathbf{p}$. Let $\mathbf{p}^* \in A_0$, suppose that the set $B_0 := B_0(\mathbf{p}^*)$ is compact,*
H16:23 *and there is a positive lower bound on the distance between $B_0$ and any point in*
H16:24 *$A_0 - B_0$.*
H16:25 *Then for every $\varepsilon > 0$ there exists a $\delta > 0$ with the following property: $\|\mathbf{p}-\mathbf{p}^*\| <$*
H16:26 *$\delta$ implies that $B_\delta(\mathbf{p})$ is contained in an $\varepsilon$-neighborhood of $B_0$.*

H16:27 The last statement simply means that $d_{\min}(\mathbf{q}, B_0) \leq \varepsilon$ for all $\mathbf{p} \in B_\delta(\mathbf{p})$, where
H16:28 $d_{\min}(\mathbf{q}, X)$ denotes the distance from $\mathbf{q}$ to the closest point in the set $X$.
H16:29 The easy proof of the lemma is given at the end. Let $\mathbf{p}^*$ be a rigid self-touching
H16:30 configuration. We apply the lemma to the sets $A_\delta$ of configurations $\mathbf{p}$ that are
H16:31 defined by relaxing the length constraints for the bars:

H16:32 $$\|\mathbf{p}_i^* - \mathbf{p}_j^*\| - 2\delta \;\leq\; \|\mathbf{p}_i - \mathbf{p}_j\| \;\leq\; \|\mathbf{p}_i^* - \mathbf{p}_j^*\| + 2\delta \quad \text{for every bar } \{i,j\}. \tag{8.1}$$

H16:33 In addition, $\mathbf{p}$ must satisfy the sidedness and noncrossing conditions of Lemma 3.1.
H16:34 Then the set $A_\delta$, viewed as a subset of the enlarged space $\mathbb{R}^{2n+4m}$ which contains
H16:35 all parameters $\bar{a}, \bar{b}, a, b$, contains all $\delta$-perturbations $\mathbf{p}$ of $\mathbf{p}^*$. By Lemma 3.1, the
H16:36 sidedness and noncrossing constraints are valid as long as $\mathbf{p}$ does not deviate by
H16:37 more than $r_0/2$ from $\mathbf{p}^*$.
H16:38 The assumption that $\mathbf{p}^*$ is rigid means that $B_0$ contains precisely the config-
H16:39 urations that are rigid motions of $\mathbf{p}^*$. To achieve compactness of $B_0$ we fix the
H16:40 position of one vertex. This can be done without changing the problem. The set
H16:41 $A_0$, being a semi-algebraic set, is locally arcwise connected, and therefore $B_0$ is the
H16:42 component of $A_0$ containing $\mathbf{p}^*$, and there is a positive lower bound on the distance
H16:43 between $B_0$ and $A_0 - B_0$. Thus, the assumptions of the lemma are fulfilled.

H17:01 The set $B_\delta(\mathbf{p})$ contains those configurations that are reachable by a weakly
H17:02 simple motion from $\mathbf{p}$. The allowed curves in $B_\delta(\mathbf{p})$ are even more relaxed, because
H17:03 the bar lengths $\|\mathbf{p}_i - \mathbf{p}_j\|$ can vary freely within the interval $\|\mathbf{p}_i^* - \mathbf{p}_j^*\| \pm 2\delta$ during
H17:04 the "motion".

H17:05 If we start a motion in any $\delta$-perturbation $\mathbf{p}$ of $\mathbf{p}^*$, we must remain inside
H17:06 $B_\delta(\mathbf{p})$, as long as $d_{\min}(\mathbf{p}, B_0) < r_0/2$. Let us choose any $\varepsilon$ with $0 < \varepsilon < r_0/2$. Then
H17:07 the lemma implies that a $\delta > 0$ exists such that starting in $\mathbf{p}$ with $\|\mathbf{p} - \mathbf{p}^*\| < \delta$
H17:08 we must always remain $\varepsilon$-close to $\mathbf{p}^*$, up to some rigid motion. This means that
H17:09 $G(\mathbf{p}^*)$ is strongly locked. □

H17:10 Proof of the lemma. We prove the lemma by contradiction. Let $\varepsilon_1 > 0$ be
H17:11 a number smaller than the minimum distance between $B_0$ and $A_0 - B_0$. Suppose
H17:12 to the contrary that, for some fixed $\varepsilon$ with $0 < \varepsilon < \varepsilon_1$ and for all $\delta$ with $0 < \delta < \varepsilon$,
H17:13 there is a point $\mathbf{p}$ with $\|\mathbf{p} - \mathbf{p}^*\| < \delta$ and a point $\bar{\mathbf{q}} \in B_\delta(\mathbf{p})$ with $d_{\min}(\bar{\mathbf{q}}, B_0) > \varepsilon$.
H17:14 We denote by $H^<$, $H^=$, and $H^>$ the set of points $x$ for which $d_{\min}(x, B_0)$ is less
H17:15 than, equal to, or bigger than $\varepsilon$. We have $\bar{\mathbf{q}} \in H^>$, and because $d_{\min}(\mathbf{p}, B_0) \leq$
H17:16 $\|\mathbf{p} - \mathbf{p}^*\| \leq \delta < \varepsilon$, we have $\mathbf{p} \in H^<$. Because $\mathbf{p}$ and $\bar{\mathbf{q}}$ are connected in $B_\delta(\mathbf{p})$ we
H17:17 can find another point $\mathbf{q} \in B_\delta(\mathbf{p}) \cap H^=$,

H17:18 Consider an infinite sequence $\delta_1, \delta_2, \ldots$ with $0 < \delta_i < \varepsilon$ converging to 0, and
H17:19 consider the corresponding sequence of points $\mathbf{p}_i$ and $\mathbf{q}_i$ with $\|\mathbf{p}_i - \mathbf{p}^*\| < \delta_i$,
H17:20 $\mathbf{q}_i \in B_{\delta_i}(\mathbf{p}_i) \subseteq A_{\delta_i}$, and $\mathbf{q}_i \in H^=$. Because the $\mathbf{q}_i$ lie in the compact set $H^=$,
H17:21 there is an infinite subsequence converging to a limit configuration $\mathbf{q}^* \in A_0 \cap H^=$,
H17:22 a contradiction. □

## H17:23 9. Proving a Linkage to be Strongly Locked

H17:24 Using the tools above, we can follow the following outline for proving that a
H17:25 particular linkage is strongly locked:

H17:26 (1) Model the linkage as a small perturbation of a self-touching linkage with
H17:27 slightly different edge lengths.
H17:28 (2) Check that the self-touching linkage is infinitesimally rigid. When the
H17:29 constraints are convex, or using the techniques in Section 6.4, this can be
H17:30 done by linear programming.
H17:31 (3) If the answer to the second step is "yes," then the self-touching linkage is
H17:32 strongly locked, and hence sufficiently close perturbations of the original
H17:33 linkage are locked within an arbitrarily small $\varepsilon$.

H17:34 The key advantage of this approach is that all but the first step is algorithmic.
H17:35 We also find that the first step typically matches the intuition of previously proposed
H17:36 examples and hence applies; the examples in the next section justify this statement.

H17:37 A limitation of the approach is that the test is conservative: an infinitesimally
H17:38 flexible linkage may still be strongly locked, and even if the self-touching linkage is
H17:39 not strongly locked, the original linkage may still be locked. In particular, the com-
H17:40 plexity of deciding whether a particular linkage is locked remains open. However,
H17:41 we find this conservative test to suffice in many examples, to which we now turn.

H17:42 To make the examples more explicit, we expand the second step into two steps
H17:43 which turn out to be easy to execute by hand, although they are slightly more
H17:44 conservative:

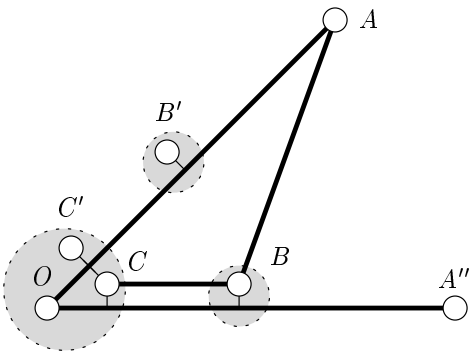


FIGURE 9. One sector of the self-touching tree from Figure 1(a). The vertices of focus form the chain $OABC$; also shown are the analog $A''$ of $A$ for the clockwise adjacent wedge, and the analogs $B', C'$ of $B$ and $C$ for the counterclockwise adjacent wedge. Thick edges denote bars, and thin edges denote sliding zero-length struts.

(2) Check whether the self-touching linkage is infinitesimally rigid:
   (a) Check that the bar version of the self-touching linkage is infinitesimally rigid.
   This step is normally quite easy because the sliding zero-length bars restrict motions severely, often creating rigid triangles.
   (b) Prove that the self-touching linkage has an equilibrium stress that is nonzero on all struts (or verify via linear programming).
   Such a stress can sometimes be constructed very easily. For example, one can superimpose stresses on simple structures like complete graphs on four vertices, where the stress is unique up to a scalar multiple. Or one can construct the stress incrementally: at a vertex of degree 3, the stress is unique up to a scalar multiple. One can start at such a vertex and establish equilibrium as one proceeds through a sequence of vertices. In the examples below, this procedure can be carried out without any computational effort, by just paying attention to the sign pattern.

If both parts succeed, then by Lemma 7.2 the self-touching linkage is infinitesimally rigid, and hence by Theorem 8.1 it is strongly locked.

Along the way, we may need to deal with touching vertices as described in Section 6.4.

## 10. Locked Trees

### 10.1. Original tree.

*Step 1*: *Model as a self-touching linkage.* Our approach applies directly to the pinwheel tree in Figure 1(a), or more precisely the self-touching version of the tree, because the ends of the arms touch the center vertex in a convex angle, and those are the only touching pairs of vertices. We focus on one sector of the pinwheel, as shown in Figure 9, and extend the stress to the whole tree by symmetry.

*Step 2(a)*: *Bar version is infinitesimally rigid.* In the bar version of the self-touching tree, $C$ is constrained to slide along both $OA$ and $OA''$, and hence $C$

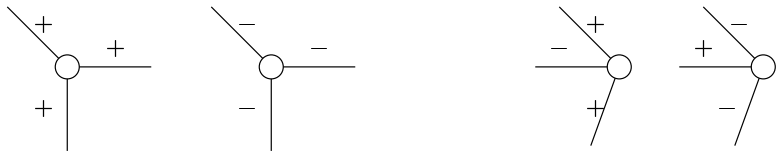


(a) 3 incident edges not in a halfplane. (b) 3 incident edges in a halfplane.

FIGURE 10. Possible sign patterns for an equilibrium stress at a degree-3 vertex when no two of the edges are collinear.

is pinned against $O$. The velocity vector $\mathbf{v}_C$ must be parallel to both $OA$ and $OA''$, and hence must be 0. Thus $OABC$ forms a rigid triangle. We get eight rigid triangles which are connected at the common vertex $O$. Because $B$ can only slide along $OA''$, the triangle $OAB$ is effectively glued to the next triangle $OA''B''$, with whom it shares the vertex $O$. So all triangles are glued together in a cyclic sequence, and the bar version is infinitesimally rigid.

*Step 2(b): Existence of equilibrium stress.* To construct the stress with the desired signs, it is helpful to imagine little springs at the struts and to think how their forces would be transmitted.

We construct the stress incrementally: A vertex with three incident stresses (not all parallel) has a unique equilibrium solution for those stresses, up to multiplication by a constant. The possible sign patterns at such a vertex are shown in Figure 10. Vertex $C$ is of type (a), so all three signs are equal. We start by giving the three edges incident to $C$ a negative stress: $\omega_{C,OA} < 0$, $\omega_{C,OA''} < 0$, and $\omega_{CB} < 0$. We balance the force from $CB$ at $B$ by two (uniquely determined) stresses $\omega_{B,OA''} < 0$, and $\omega_{BA} < 0$. We repeat these stresses symmetrically for all sections around the wheel. By symmetry, this will establish equilibrium at $O$. We now still have unresolved forces at $A$ and the analogous vertices $A', A'', \ldots$. The direction of the force at $A$ must be parallel to $OA$ because otherwise all the forces would generate a nonzero rotational moment around $O$. This is impossible, because individual forces generated by the stresses $\omega_{ij}$ and $\omega_{k,ij}$ are torque-free. Thus the forces at $A$ (and $A', \ldots$) can be canceled by stresses $\omega_{OA} > 0$, without destroying equilibrium at $O$. This stress is negative on all struts.

*Step 3: Finale.* By Lemma 7.2, the self-touching linkage is infinitesimally rigid, so by Lemma 6.1 it is also rigid, so by Theorem 8.1 it is also strongly locked. Hence, if the original tree in Figure 1(a) is drawn sufficiently tight, then it is locked within some small $\varepsilon$.

Given the setup from the previous sections, this proof is simpler than the original proof that this tree is locked [**BDD+02**].

### 10.2. New tree.

*Step 1: Model as self-touching linkage.* To apply the approach to the tree in Figure 1(c) in a similarly easy way, we drop some of the struts; see Figure 11. If we can show that the linkage with fewer struts is infinitesimally rigid, the original linkage must also be infinitesimally rigid. Again, we exploit symmetry and focus on one portion of the linkage.

*Step 2(a): Bar version is infinitesimally rigid.* $C$ is constrained to slide along both $OA$ and $OA''$, and hence $C$ is stuck at $O$. The same argument holds for $G$ and $G''$. The sliding struts between $B$ and $D$, and between $D$ and $F''$, perpendicular to

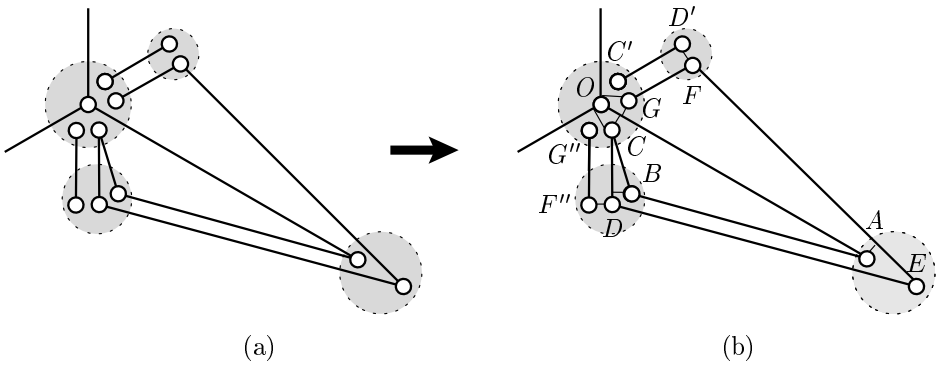


FIGURE 11. One arm of the tree in Figure 1(c). The vertices of focus form the chain $OABCDEFG$; also shown are the analogs $F'', G''$ of $F, G$ for the clockwise adjacent wedge, and the analogs $C', D'$ of $C, D$ for the counterclockwise adjacent wedge. Thick edges denote bars, and thin edges denote sliding zero-length struts. Only the struts which are used to prove rigidity are shown.

$CD$ now hold $B$, $D$ and $F''$ together. Thus $OABDC$ forms a rigid triangle, with $O = A$ and $B = D$. If we regard this triangle as fixed, the bar $DE$ constrains the infinitesimal motion of $E$ to directions perpendicular to $DE$, whereas the sliding strut which keeps $A$ on $EF$ restrains the relative motion of $A$ and $E$ to directions parallel to $EF$. This prevents any relative motion of $E$ with respect to $A$, making the triangle $OAEFG$ rigid too. So we get a rigid structure of six triangles glued together around $O$ in a cyclic fashion.

*Step 2(b): Existence of equilibrium stress.* We will construct a stress which is negative on all struts. For simplicity, we write $\omega_{BD}$ for the stress between $B$ and $D$ in the direction perpendicular to $OB$. This stress can be interpreted as $\omega_{B,CD}$, as suggested by the figure, or as $\omega_{D,BC}$; it does not matter which. Similarly, we will use $\omega_{DF''}$ and $\omega_{D'F}$.

We start with an equilibrium at $F$ by giving the three incident edges a negative stress: $\omega_{FG} < 0$, $\omega_{EF} < 0$, and $\omega_{D'F} < 0$. The negative force at $G$ can be canceled by negative stresses $\omega_{G,OA} < 0$ and $\omega_{G,OA'} < 0$. Now $E$ has two more edges besides $EF$; we create equilibrium at $E$ by setting $\omega_{A,EF} < 0$ and $\omega_{DE} > 0$. (To see the correct sign pattern, one must draw the sliding strut with stress $\omega_{A,EF} < 0$ attached to $E$ and not to $A$ as in the figure.)

All of this is of course done symmetrically in the three arms of the tree. So the vertex $D$ already has a stress $\omega_{DF''} < 0$ which is determined, in addition to $\omega_{DE} > 0$ which we just fixed. The resulting force induces a unique solution for $\omega_{BD}$ and $\omega_{CD}$. We can find this solution in two steps. First we ignore $\omega_{DF''}$ and get an equilibrium with $\omega_{DE} > 0$, $\omega^0_{BD} < 0$, and $\omega_{CD} > 0$. Now $\omega_{DF''} < 0$ can be canceled by further decreasing $\omega_{BD}$ to its final value $\omega^1_{BD} < \omega^0_{BD} < 0$. We extend $\omega^1_{BD} < 0$ to an equilibrium at $B$ by setting $\omega_{BC} < 0$ and $\omega_{AB} < 0$. The situation in $B$ is almost the same as in $D$ when we first constructed the equilibrium in $B$ with the initial value $\omega^0_{BD}$: the three edges point in parallel directions and have the same lengths. The difference is that $\omega_{BD}$ points in the opposite direction when

seen from $B$, and $|\omega^1_{BD}| > |\omega^0_{BD}|$. It follows for the corresponding parallel edges $CD$ and $BC$ that $|\omega_{BC}| > |\omega_{CD}|$.

Therefore, in $C$, the negative stress $\omega_{BC}$ prevails over the positive stress $\omega_{CD}$, resulting in a negative total force in $C$ from the direction of $B$ and $D$: $\omega_{BC}+\omega_{CD} < 0$. This force is canceled by negative stresses $\omega_{C,OA} < 0$ and $\omega_{C,OA''} < 0$.

We can now conclude as for the simple tree. By symmetry, $O$ must be in equilibrium, and the three remaining forces in $A$, $A'$, and $A''$ must be parallel to $OA$, $OA'$, and $OA''$, respectively, so they can be canceled by appropriate stresses on those edges.

*Step 3: Finale.* By Lemma 7.2, the self-touching linkage is infinitesimally rigid, so by Lemma 6.1 it is also rigid, so by Theorem 8.1 it is also strongly locked. Hence, if the original tree in Figure 1(c) is drawn sufficiently tight, then it is locked within an arbitrarily small $\varepsilon$. In the appendix we show that any $\delta$-perturbation of the tree is locked within 0.0001, for $\delta = 3 \times 10^{-8}$.

## 11. Conclusion

To study when linkages are locked, we developed the notion of a *self-touching* linkage which captures instantaneous crossing constraints. We then generalized rigidity theory to capture such noncrossing constraints, the difficulty being that in some cases the constraints are nonconvex. We proved that rigidity in this setting implies that the linkage is *strongly locked*, meaning that small enough perturbations of the linkage can barely move, as little as desired. In particular, this brings results about self-touching linkages into the commonly studied realm of strictly simple, nontouching linkages.

Our theory can be used to prove a variety of linkages to be strongly locked. In particular, we showed two examples here: the tree from [**BDD+02**], and a new tree with a single degree-3 vertex.

## References


[AR78] L. Asimow and B. Roth, *The rigidity of graphs*, Transactions of the American Mathematical Society **245** (1978), 279–289.

[AR79] L. Asimow and B. Roth, *The rigidity of graphs. II*, Journal of Mathematical Analysis and Applications **68** (1979), no. 1, 171–190.

[BDD+02] Therese Biedl, Erik Demaine, Martin Demaine, Sylvain Lazard, Anna Lubiw, Joseph O'Rourke, Steve Robbins, Ileana Streinu, Godfried Toussaint, and Sue Whitesides, *A note on reconfiguring tree linkages: Trees can lock*, Discrete Applied Mathematics **117** (2002), 293–297. The full version is Technical Report SOCS-00.7, School of Computer Science, McGill University, September 2000, and Computing Research Repository paper cs.CG/9910024. `http://www.arXiv.org/abs/cs.CG/9910024`.

[Can87] John Canny, *A new algebraic method for robot motion planning and real geometry*, Proceedings of the 28th Annual Symposium on Foundations of Computer Science (Los Angeles, California), October 1987, IEEE Computer Society Press, Washington, D.C., 1987, pp. 39–48.

[Can88] John Canny, *Some algebraic and geometric computations in PSPACE*, Proceedings of the 20th Annual ACM Symposium on Theory of Computing (Chicago, Illinois), May 1988, ACM Press, New York, 1988, pp. 460–469.

[CDR02] Robert Connelly, Erik D. Demaine, and Günter Rote, *Straightening polygonal arcs and convexifying polygonal cycles*, Discrete & Computational Geometry, to appear. Preliminary version in the Proceedings of the 41st Annual Symposium on Foundations of Computer Science (Redondo Beach, California), November 2000, IEEE Computer Society Press, Washington, D.C., 2000, pp. 432–442; an extended version is available as Technical report B 02-02, Freie Universität Berlin, Institut für Informatik, 2002.

[Con80] Robert Connelly, *The rigidity of certain cabled frameworks and the second-order rigidity of arbitrarily triangulated convex surfaces*, Advances in Mathematics **37** (1980), no. 3, 272–299.

[Con82] Robert Connelly, *Rigidity and energy*, Inventiones Mathematicae **66** (1982), no. 1, 11–33.

[Con93] Robert Connelly, *Rigidity*, in: Handbook of Convex Geometry, vol. A (Peter M. Gruber and Jörg M. Wills, eds.), North-Holland, Amsterdam, 1993, pp. 223–271.

[CW82] Henry Crapo and Walter Whiteley, *Statics of frameworks and motions of panel structures, a projective geometric introduction (with a French translation)*, Structural Topology **6** (1982), 43–82.

[CW93] Henry Crapo and Walter Whiteley, *Autocontraintes planes et polyèdres projetés. I. Le motif de base [Plane self stresses and projected polyhedra. I. The basic pattern]*, Structural Topology **20** (1993), 55–78.

[CW94] Henry Crapo and Walter Whiteley, *Spaces of stresses, projections and parallel drawings for spherical polyhedra*, Beiträge zur Algebra und Geometrie **35** (1994), no. 2, 259–281.

[CW96] Robert Connelly and Walter Whiteley, *Second-order rigidity and prestress tensegrity frameworks*, SIAM Journal on Discrete Mathematics **9** (1996), no. 3, 453–491.

[Dem00] Erik D. Demaine, *Folding and unfolding linkages, paper, and polyhedra*, in: Discrete and Computational Geometry (Jin Akiyama, Mikio Kano, and Masatsugu Urabe, eds.), Revised Papers from the Japan Conference on Discrete and Computational Geometry (Tokyo, Japan), JCDCG 2000, Lecture Notes in Computer Science, vol. 2098, Springer-Verlag, 2001, pp. 113–124.

[GSS93] Jack Graver, Brigitte Servatius, and Herman Servatius, *Combinatorial rigidity*, American Mathematical Society, Providence, 1993.

[Mil68] John Milnor, *Singular points of complex hypersurfaces*, Princeton University Press, 1968.

[O'R98] Joseph O'Rourke, *Folding and unfolding in computational geometry*, in: Discrete and Computational Geometry (Jin Akiyama, Mikio Kano, and Masatsugu Urabe, eds.), Revised Papers from the Japan Conference on Discrete and Computational Geometry (Tokyo, Japan), JCDCG'98, December 1998, Lecture Notes in Computer Science, vol. 1763, Springer-Verlag, 2000, pp. 258–266.

[RW81] B. Roth and W. Whiteley, *Tensegrity frameworks*, Transactions of the American Mathematical Society **265** (1981), no. 2, 419–446.

[Str00] Ileana Streinu, *A combinatorial approach to planar non-colliding robot arm motion planning*, Proceedings of the 41st Annual Symposium on Foundations of Computer Science (Redondo Beach, California), November 2000, IEEE Computer Society Press, Washington, D.C., 2000, pp. 443–453.

[Whi84a] Walter Whiteley, *Infinitesimally rigid polyhedra. I. statics of frameworks*, Transactions of the American Mathematical Society **285** (1984), no. 2, 431–465.

[Whi84b] Walter Whiteley, *The projective geometry of rigid frameworks*, in: Finite geometries (Catherine Anne Baker and Lynn Margaret Batten, eds.) Proc. Conf. Winnipeg, 1984, Lecture Notes in Pure and Applied Mathematics, vol. 103, Marcel Dekker, New York–Basel, 1985, pp. 353–370.

[Whi87] Walter Whiteley, *Rigidity and polarity. I. Statics of sheet structures*, Geometriae Dedicata **22** (1987), no. 3, 329–362.

[Whi88] Walter Whiteley, *Infinitesimally rigid polyhedra. II. Modified spherical frameworks*, Transactions of the American Mathematical Society **306** (1988), no. 1, 115–139.

[Whi92] Walter Whiteley, *Matroids and rigid structures*, Matroid applications (Neil White, ed.), Encyclopedia of Mathematics and its Applications, vol. 40, Cambridge University Press, Cambridge, 1992, pp. 1–52.

## Appendix A. Constructive Proof of Theorem 8.1

Here we prove another version of Theorem 8.1. We have to make the stronger assumption of *infinitesimal* rigidity, but the proof gives a way to compute $\delta$ in terms of $\varepsilon$.

H23:01 THEOREM A.1. *If a self-touching linkage is infinitesimally rigid, then it is*
H23:02 *strongly locked.*

H23:03 PROOF. Let $\mathbf{p}^* = (\mathbf{p}_1^*, \dots, \mathbf{p}_n^*)$ be an infinitesimally rigid self-touching linkage.
H23:04 We select an edge, say $\mathbf{p}_1\mathbf{p}_2$, and fix its position by setting $\mathbf{v}_1 = \mathbf{v}_2 = 0$. Infini-
H23:05 tesimal rigidity means that the system $\mathcal{M}$ has only the trivial solution. We apply
H23:06 Lemma 6.2(2) and get a family of linear systems $\mathcal{M}_1, \mathcal{M}_2, \dots$, all of which have
H23:07 only the trivial solution. Each system $\mathcal{M}_g$ has the form

H23:08 $$\mathbf{v}_1 = \mathbf{v}_2 = 0 \tag{A.1}$$

H23:09 $$\mathbf{v}_j \cdot (\mathbf{p}_j^* - \mathbf{p}_i^*) - \mathbf{v}_i \cdot (\mathbf{p}_j^* - \mathbf{p}_i^*) = 0 \tag{A.2}$$

H23:10 $$-\mathbf{v}_k \cdot (\mathbf{p}_j^* - \mathbf{p}_i^*)^\perp + \alpha \mathbf{v}_i \cdot (\mathbf{p}_j^* - \mathbf{p}_i^*)^\perp + (1-\alpha)\mathbf{v}_j \cdot (\mathbf{p}_j^* - \mathbf{p}_i^*)^\perp \le 0 \tag{A.3}$$

H23:11 (for all bars $i, j$ and certain triples $i, j, k$, and certain $\alpha = \alpha_{ijk}$, $0 \le \alpha \le 1$)

H23:12 LEMMA A.2. *Assume $0 \le \delta \le \varepsilon \le r_1/2$, where $r_1$ is the minimum positive*
H23:13 *distance between two vertices or between a vertex and an edge in a given configura-*
H23:14 *tion $\mathbf{p}^*$. Let $\mathbf{p}^1$ be a $\delta$-perturbation of $\mathbf{p}^*$:*

H23:15 $$\|\mathbf{p}^1 - \mathbf{p}^*\| \le \delta,$$

H23:16 *and consider a path $\mathbf{p}(t) \in \mathbb{R}^{2n}$, $0 \le t \le T$, in the configuration space with $\mathbf{p}(0) =$*
H23:17 *$\mathbf{p}^1$, with*

H23:18 $$\|\mathbf{p}(t) - \mathbf{p}^*\| < \varepsilon, \text{ for all } 0 \le t \le T$$

H23:19 *Then, for all $\mathbf{p} = \mathbf{p}(t)$, there is a system $\mathcal{M}_g$ in which the equations and inequalities*
H23:20 (A.2–A.3) *hold for $\mathbf{p}_i - \mathbf{p}_i^*$ instead of $\mathbf{v}_i$, with a fudge factor $C_1\delta + C_2\varepsilon^2$, where*
H23:21 *$C_2 = 4$ and $C_1$ depends only on $\mathbf{p}^*$. More precisely,*

H23:22 $$-[2\|\mathbf{p}_j^* - \mathbf{p}_i^*\| \cdot \delta + 4\varepsilon^2] \le \ell_{ij} \le 2\|\mathbf{p}_j^* - \mathbf{p}_i^*\| \cdot \delta \tag{A.4}$$

H23:23 $$\text{with } \ell_{ij} := (\mathbf{p}_j - \mathbf{p}_j^*) \cdot (\mathbf{p}_j^* - \mathbf{p}_i^*) - (\mathbf{p}_i - \mathbf{p}_i^*) \cdot (\mathbf{p}_j^* - \mathbf{p}_i^*),$$

H23:24 *and*

H23:25 $$-(\mathbf{p}_k - \mathbf{p}_k^*) \cdot (\mathbf{p}_j^* - \mathbf{p}_i^*)^\perp \tag{A.5}$$

H23:26 $$+\alpha(\mathbf{p}_i - \mathbf{p}_i^*) \cdot (\mathbf{p}_j^* - \mathbf{p}_i^*)^\perp + (1-\alpha)(\mathbf{p}_j - \mathbf{p}_j^*) \cdot (\mathbf{p}_j^* - \mathbf{p}_i^*)^\perp \le 4\varepsilon^2.$$

H23:27 PROOF. The idea of the proof is as follows: By Lemma 3.2, $\mathbf{p}(t)$ must fulfill a set
H23:28 of noncrossing and sidedness conditions. When we write these sidedness condition
H23:29 for $\mathbf{p}$, we get almost (A.5), except that we take the inner product with $(\mathbf{p}_j^* - \mathbf{p}_i^*)^\perp$
H23:30 instead of $(\mathbf{p}_j - \mathbf{p}_i)^\perp$. For small $\varepsilon$, these two directions are almost parallel, and the
H23:31 difference is $O(\varepsilon^2)$. For the length-preserving condition there is an additional term
H23:32 of $O(\delta)$ because the length of the bar can change by up to $2\delta$.
H23:33 To prove (A.4), we have to bound the difference $\Delta$ between

H23:34 $$(\mathbf{p}_j - \mathbf{p}_i) \cdot (\mathbf{p}_j^* - \mathbf{p}_i^*) = \|\mathbf{p}_j - \mathbf{p}_i\| \cdot \|\mathbf{p}_j^* - \mathbf{p}_i^*\| \cdot \cos\varphi$$

H23:35 and

H23:36 $$(\mathbf{p}_j^* - \mathbf{p}_i^*) \cdot (\mathbf{p}_j^* - \mathbf{p}_i^*) = \|\mathbf{p}_j^* - \mathbf{p}_i^*\| \cdot \|\mathbf{p}_j^* - \mathbf{p}_i^*\|,$$

H23:37 where $\varphi$ is the angle between $\mathbf{p}_j - \mathbf{p}_i$ and $\mathbf{p}_j^* - \mathbf{p}_i^*$.

H23:38 $$\Delta = \|\mathbf{p}_j^* - \mathbf{p}_i^*\| \cdot \left(\|\mathbf{p}_j - \mathbf{p}_i\| \cdot \cos\varphi - \|\mathbf{p}_j^* - \mathbf{p}_i^*\|\right).$$

H24:01 For bounding the right-hand side, we know that $\|\mathbf{p}_j - \mathbf{p}_i\|$ is bounded between
H24:02 $\|\mathbf{p}_j^* - \mathbf{p}_i^*\| \pm 2\delta$, and

H24:03 $$1 \geq \cos\varphi \geq \sqrt{1 - \left(\frac{2\varepsilon}{\|\mathbf{p}_j^* - \mathbf{p}_i^*\|}\right)^2} \geq 1 - \frac{4\varepsilon^2}{\|\mathbf{p}_j^* - \mathbf{p}_i^*\|^2}.$$

H24:04 Plugging this in gives the desired relation.

H24:05 Proof of (A.5): We have

H24:06 $$\mathbf{p}_k^* = \alpha\mathbf{p}_i^* + (1-\alpha)\mathbf{p}_j^*$$

H24:07 The corresponding point

H24:08 $$\bar{\mathbf{p}}_k := \alpha\mathbf{p}_i + (1-\alpha)\mathbf{p}_j$$

H24:09 lies on the line segment $\mathbf{p}_i\mathbf{p}_j$ and inside the $\varepsilon$-circle around $\mathbf{p}_k$.

H24:10 We have

H24:11 $$-\mathbf{p}_k^* \cdot (\mathbf{p}_j^* - \mathbf{p}_i^*)^\perp + \alpha\mathbf{p}_i^* \cdot (\mathbf{p}_j^* - \mathbf{p}_i^*)^\perp + (1-\alpha)\mathbf{p}_j^* \cdot (\mathbf{p}_j^* - \mathbf{p}_i^*)^\perp = 0$$

H24:12 and

H24:13 $$-\bar{\mathbf{p}}_k \cdot (\mathbf{p}_j^* - \mathbf{p}_i^*)^\perp + \alpha\mathbf{p}_i \cdot (\mathbf{p}_j^* - \mathbf{p}_i^*)^\perp + (1-\alpha)\mathbf{p}_j \cdot (\mathbf{p}_j^* - \mathbf{p}_i^*)^\perp = 0.$$

H24:14 The difference between these two terms is almost what we want in (A.5), except
H24:15 that we have to replace $\bar{\mathbf{p}}_k$ by $\mathbf{p}_k$. The point $\mathbf{p}_k$ lies also inside the $\varepsilon$-circle around
H24:16 $\mathbf{p}_k$ and *above* the line segment $\mathbf{p}_i\mathbf{p}_j$. So

H24:17 $$(\mathbf{p}_k - \bar{\mathbf{p}}_k) \cdot (\mathbf{p}_j^* - \mathbf{p}_i^*)^\perp \geq -2\varepsilon \cdot \|\mathbf{p}_j^* - \mathbf{p}_i^*\| \sin\varphi,$$

H24:18 where $\varphi$ is the angle between $\mathbf{p}_j - \mathbf{p}_i$ and $\mathbf{p}_j^* - \mathbf{p}_i^*$. We have

H24:19 $$\sin\varphi \leq \frac{\varepsilon}{\sqrt{(\|\mathbf{p}_j^* - \mathbf{p}_i^*\|/2)^2 - \varepsilon^2}} \leq \frac{\varepsilon}{\|\mathbf{p}_j^* - \mathbf{p}_i^*\|/2},$$

H24:20 and this gives

H24:21 $$(\mathbf{p}_k - \bar{\mathbf{p}}_k) \cdot (\mathbf{p}_j^* - \mathbf{p}_i^*)^\perp \geq -4\varepsilon^2.$$ □

H24:22 Lemma A.3. *Assume that the system $Av \leq 0$ has only the solution $v = 0$.*
H24:23 *Then for any $\gamma \geq 0$, every solution of $Av \leq \gamma$ (componentwise) has $\|v\| \leq C_3\gamma$, for*
H24:24 *some constant $C_3$ depending only on $A$.*

H24:25 Proof. The polyhedron $Av \leq 1$ is bounded, and $C_3$ is the distance of its
H24:26 farthest vertex from the origin. □

H24:27 Finally we prove that $\mathbf{p}^*$ is locked within $\varepsilon$. Let $C_3$ be a constant for Lemma A.3
H24:28 such that $\|v\| \leq C_3\gamma$ holds, for the coefficient matrices $A$ of the systems (A.1–A.3)
H24:29 of all systems $\mathcal{M}_g$. Assume that $\mathbf{p}^1$ and $\mathbf{p} = \mathbf{p}(t)$ are as in Lemma A.2 with
H24:30 $\varepsilon := 1/(3C_2C_3)$ and $\delta := 1/(9C_1C_2C_3^2) = \frac{\varepsilon}{3C_1C_3}$. By choosing a larger constant $C_3$
H24:31 if necessary we can assure that $\delta$ and $\varepsilon$ satisfy the assumptions of Lemma A.2, and
H24:32 by choosing a larger constant $C_2$ we can ensure that $\varepsilon$ is smaller than any given
H24:33 desired value.

H24:34 Then we know that $v = \mathbf{p} - \mathbf{p}^*$ fulfills $Av \leq \gamma$ with

H24:35 $$\gamma = C_1\delta + C_2\varepsilon^2 = \frac{2}{9} \cdot \frac{1}{C_2C_3^2}$$

H24:36 and, by Lemma A.3, this implies $\|\mathbf{p}_i - \mathbf{p}_i^*\| \leq C_3\gamma = \frac{2}{9} \cdot \frac{1}{C_2C_3} = \frac{2}{3}\varepsilon$.

It follows that $\mathbf{p}$ cannot possibly reach any position with

$$\tfrac{2}{3}\varepsilon < \max_i \|\mathbf{p}_i - \mathbf{p}_i^*\| \leq \varepsilon.$$

Thus each point $\mathbf{p}_i$ is confined within a disk of radius $\frac{2}{3}\varepsilon$ around $\mathbf{p}_i^*$. □

To compute the value of $\delta$ for a given $\varepsilon$, we have to know the constants $C_1$, $C_2$, $C_3$, and $r_1$. We have $C_2 = 4$ and $C_1 = 2D_{\max}$, where $D_{\max}$ is the length of the longest bar. These are geometric quantities of the configuration. The constant $C_3$ is harder to compute. We can approximate it by computing the axes-parallel bounding box of the polytope $Av \leq 1$, solving $O(n)$ linear programming problems. The size of this polytope measures how "rigid" the linkage is, in terms of sensitivity to tolerances in the edge lengths. Edges that are almost parallel where they meet will in general lead to a large polytope.

If we draw the tree in Figure 1(c) symmetrically and put $OA = 1$ and $OB = 1/3$ (in the notation of Figure 11b), we get $C_1 = 2$ and $C_3 \leq 634$, using the norm (3.1). By plugging these values into the formulas, one obtains that any $\delta$-perturbation of the tree is locked within $\varepsilon$, for $\delta = 3 \times 10^{-8}$ and $\varepsilon = 0.0001$. One can slightly improve these formulas by balancing $\delta$ and $\varepsilon$ in the derivation. A direct, but tedious proof reveals that the tree is locked for $\delta = 0.00005$, but unlocked for $\delta = 0.001$.

Department of Mathematics, Cornell University, Ithaca, NY 14853, U.S.A.
*E-mail address*: connelly@math.cornell.edu

MIT Laboratory for Computer Science, 200 Technology Square, Cambridge, MA 02139, U.S.A.
*E-mail address*: edemaine@mit.edu

Institut für Informatik, Freie Universität Berlin, Takustrasse 9, D-14195 Berlin, Germany
*E-mail address*: rote@inf.fu-berlin.de